

Genetically Encoded Oligomerization for Protein-Based Lighting Devices

Marta Patrian, Mattia Nieddu, Jesús A. Banda-Vázquez, David Gutierrez-Armayor, Gustavo González-Gaitano, Juan Pablo Fuenzalida-Werner,* and Rubén D. Costa*

Implementing proteins in optoelectronics represents a fresh idea toward a sustainable new class of materials with bio-functions that can replace environmentally unfriendly and/or toxic components without losing device performance. However, their native activity (fluorescence, catalysis, and so on) is easily lost under device fabrication/operation as non-native environments (organic solvents, organic/inorganic interfaces, and so on) and severe stress (temperature, irradiation, and so on) are involved. Herein, a gift bow genetically-encoded macro-oligomerization strategy is showcased to promote protein–protein solid interaction enabling i) high versatility with arbitrary proteins, ii) straightforward electrostatic driven control of the macro-oligomer size by ionic strength, and iii) stabilities over months in pure organic solvents and stress scenarios, allowing to integrate them into classical water-free polymer-based materials/components for optoelectronics. Indeed, rainbow-/white-emitting protein-based light-emitting diodes are fabricated, attesting a first-class performance compared to those with their respective native proteins: significantly enhanced device stabilities from a few minutes up to 100 h keeping device efficiency at high power driving conditions. Thus, the oligomerization concept is a solid bridge between biological systems and materials/components to meet expectations in bio-optoelectronics, in general, and lighting schemes, in particular.

programmed to optimize their bio-functionality (fluorescence, redox behaviors, catalytic activity, transport phenomena, and so on) in living systems. While protein engineering and synthetic biology have mastered an excellent genetic toolbox, enabling the tuning of protein functionality in vivo with high relevance in medicine (imaging, biosensors, etc.),^[1,2] their stabilization with respect to their natural functions outside of their native environments (aqueous solutions with controlled pH, ionic strength, and temperature) has been unsuccessful, limiting the progress of the emerging field of protein-based materials and optoelectronic.^[3–8] Here, the challenge is twofold: i) device fabrication using traditional techniques (organic solvent deposition techniques, inert atmospheres, and so on) and architectures (organic/inorganic interfaces, electrodes, water-free environments, and so on), as well as ii) operating conditions (in-/out-door temperature and irradiation stress, dry/inert atmosphere, and so on).

In this context, leading concepts in protein/enzyme stabilization in non-aqueous

environments are divided into two main categories: i) isolation strategies, such as reverse micelles, sol–gel chemistry, chemical modification, and use of random heteropolymers,^[9–13] which shield them from the surrounding denaturing environment, and ii) genetically encoded approaches, such as directed evolution and engineered inclusion bodies,^[14–22] that modify them increasing their resistance to the hostile environment. On the one hand, isolation strategies via reverse micelles led to up to 24 h stabilities only in mixed organic-aqueous solvents.^[12] Sol–gel chemistry achieved function retention (80%) up to 5 days in pure organic solvents but risking both enzyme inactivation and end material optical and mechanical properties.^[13] In addition, surface polymer decoration relies on the need of specific amino acidic residues and has featured a low compatibility with polymer composites of relevance for optoelectronics.^[10] The use of random heteropolymers has also stabilized proteins in organic solvents for a short period of up to 25 h.^[11] On the other hand, directed evolution, which led to improved stabilities in diluted organic solvents,^[14–19] cannot be generalized to pure organic solvents, polymer environments, and device interfaces. Finally, genetically induced incorporation in inclusion bodies results in partially

1. Introduction

Proteins and enzymes are a paradigm of smart materials, in which chemical diversity and hierarchical structure are

M. Patrian, M. Nieddu, J. A. Banda-Vázquez, D. Gutierrez-Armayor, J. P. Fuenzalida-Werner, R. D. Costa
Chair of Biogenic Functional Materials
Technical University of Munich
Schulgasse, 22, 94315 Straubing, Germany
E-mail: jpf.werner@tum.de; ruben.costa@tum.de

G. González-Gaitano
Departamento de Química
Universidad de Navarra
Pamplona 31080, Spain

 The ORCID identification number(s) for the author(s) of this article can be found under <https://doi.org/10.1002/adma.202303993>

© 2023 The Authors. Advanced Materials published by Wiley-VCH GmbH. This is an open access article under the terms of the Creative Commons Attribution-NonCommercial License, which permits use, distribution and reproduction in any medium, provided the original work is properly cited and is not used for commercial purposes.

DOI: 10.1002/adma.202303993

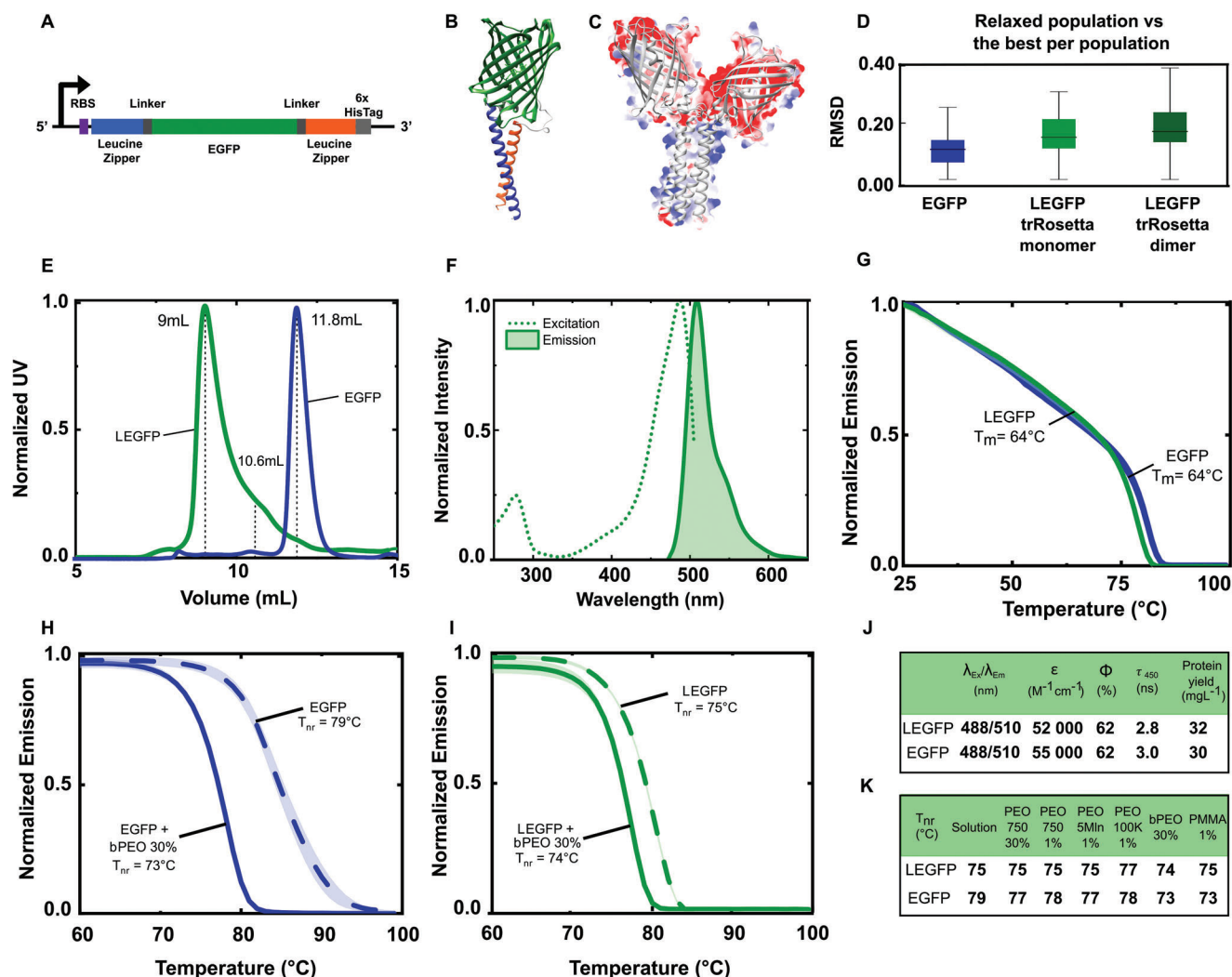


Figure 1. Characterization of LEGFP. A) LEGFP genetic construct. B) AlphaFold2 model of monomeric LEGFP; the leucine zipper region is indicated in blue (N-terminal) and orange (C-terminal). C) Superposition of LEGFP dimer (grey ribbons) with its colubric surface coloring. D) EGFP, LEGFP monomer, and LEGFP dimer root-mean-square deviation (RMSD) analysis of Rosetta minimized populations. E) SEC of LEGFP and EGFP; dotted lines indicate the volumes of elution LEGFP dimer, LEGFP monomer, and EGFP. F) Excitation and emission spectra of LEGFP. G) Melting temperature (T_m) of LEGFP and EGFP. H, I) Non-reversible folding temperatures (T_{nr}) of EGFP and LEGFP in the presence and absence of bPEO 30%. J) Overview of LEGFP and EGFP main photophysical properties and production yields. K) Graphical overview of LEGFP and EGFP non-reversible folding temperatures in the presence and absence of synthetic polymers.

unfolded proteins along with other cell components, exhibiting a tradeoff in processability, accessibility, and loss of native function of up to 85%.^[22] Unfortunately, none of these strategies has shown to be effective to integrate proteins/enzymes as active components in energy-related bio-optoelectronic devices yet.

Herein, we capitalize on a purely electrostatic driving force to promote protein–protein interactions fusing the N and C terminus of arbitrary fluorescent proteins (FPs); enhanced green fluorescent protein or EGFP and mNeptune2.5) with antiparallel leucine zippers in a gift bow fashion (Figure 1). The engineered constructs allowed us to easily generate FP-based macro-oligomers via simple ionic strength change, controlling size distribution and protein selectivity. This versatile concept led to highly emissive macro-oligomers with an excellent stability in pure organic solvents (>3 months) and stress scenarios com-

pared to both their respective native FPs and the prior-art (vide supra). What is more, this allowed us to easily implement them in a myriad of water-processed and water-free polymer composites commonly applied to develop bio-hybrid light-emitting diodes (Bio-HLEDs). This technology promises to satisfy Europe and US regulatory agencies' priorities for eco-friendly and sun-like illumination technologies.^[23–25] In short, the lighting market is dominated by inorganic white light-emitting diodes (WLEDs) based on inorganic phosphors (IPs) such as unsustainable Ce-doped $Y_3Al_5O_{12}$ (YAG:Ce) or toxic Cd-based quantum dots (CdQDs) employed in commercial WLEDs and displays. Thus, extensive research is being done on hybrid light-emitting diodes (HLEDs), in which organic color down-converting filters based on small molecules, conjugated polymer, coordination complexes, and so on, embedded into polymer/epoxy are

investigated.^[7,26–31] Among them, FPs are considered a model of sustainability with respect to their cheap bacterial production, easy recyclability, water-processability, excellent emission merits, and low-cost as high purification levels are not required.^[32–35] In addition, the performance of Bio-HLEDs is becoming more and more appealing with stabilities of >3000 h and efficiencies of >130 lm W⁻¹ at low-power conditions (<50 mW cm⁻² photon flux excitation)^[7] compared to other devices with traditional organic phosphors: i) perylene diimide-polymer with <700 h@130 lm W⁻¹,^[29] ii) BODIPYs-polymer with <10 h@13 lm W⁻¹,^[31] and iii) Iridium(III) complex-polymer with <1000 h@100 lm W⁻¹.^[30] In contrast, the device stability is typically reduced to <5 min at high-power operation conditions (200 mW cm⁻² photon-flux excitation; due to photo-induced heat generation (up to 70 °C) in the color down-converting coating caused by FP motion and efficient heat transfer in a water-rich environment.^[6,7] In this work, rainbow- and white-emitting Bio-HLEDs with FP-based macro-oligomers operating at photon flux excitation of 200 mW cm⁻² featured significantly enhanced stabilities of up to 100 h due to the lack of heat generation in water-free coatings, resulting in first-class devices.^[4–7] Thus, the oligomerization concept makes closer the development of sustainable protein-based optoelectronics, bridging the worlds of protein and device engineering.

2. Results and Discussion

2.1. Genetically Encoded FP Macro-Oligomerization

As the N and C terminus are facing the same side of the typical β -barrel structure of FPs, a complementary pair of leucine zippers were genetically attached to this flexible region of EGFP to increase protein's surface and block the β -barrel's unfolding by restricting the motions of the flexible ends (Figure 1A,B). More importantly, the leucine zippers were selected to bear a high number of complementary exposed charges to promote strong interactions between monomers. Rosetta minimization^[36] on AlphaFold2^[37] models of the leucine zipper EGFP protein (LEGFP) showed no negative effect on conformational stability in comparison to EGFP, confirming a preference for a dimeric conformation with predicted interface interaction in the range of natural FP dimers (Figure 1B–D; Table S1, Supporting Information).

LEGFP production in *Escherichia coli* is similar to EGFP (Figure 1J) and can be purified via affinity chromatography and size exclusion chromatography (SEC), confirming similar levels of protein solubility. Analytical SEC analysis corroborated the oligomeric AlphaFold2 model, showing that LEGFP elutes mostly as a dimer in standard PBS buffer (Figure 1E). The absorption extinction coefficient (ϵ), fluorescent quantum yield (ϕ), and excitation/emission spectra are the same for LEGFP and EGFP, indicating that our modification did not alter the chromophore environment (Figure 1F,J). The excited state lifetime (τ) of LEGFP (2.8 ns) is; however, shorter than that of EGFP (3.0 ns) caused by the higher refractive index of the neighboring proteins in its dimeric conformation.^[38]

The dynamic/static stability of LEGFP was studied using modulated scanning fluorimetry (MSF). While both proteins share a melting point of 69 °C (T_m -50%; Figure 1G), LEGFP features a lower non-reversibility temperature compared to EGFP

(T_{nr} ; Figure 1H,I). Conversely, the leucine zippers confer better thermodynamic parameters to LEGFP in the presence of synthetic polymers used in bio-hybrid light-emitting diodes (Bio-HLEDs).^[4–7] Upon addition of the archetypal branched polyethylene oxide (bPEO), LEGFP showed a slight change in T_{nr} from 75 °C to 74 °C, while EGFP refolding capability is reduced from 79 °C to 73 °C (Figure 1H,I). To confirm the superior stability of LEGFP in various polymers, we performed MSF of protein solution with polymethyl methacrylate (PMMA) and PEOs of different molecular weights ranging from 750 to 5 000 000. In all the cases, the T_{nr} of LEGFP remained mostly unaffected, while the T_{nr} of EGFP was negatively impacted (Figure 1K; Figure S1, Supporting Information). The denaturing effects of synthetic polymers are mainly ascribed to their direct interaction with hydrophobic patches in the protein backbone, forcing a change in protein conformation.^[39] Thus, the larger volume and the dimeric character of LEGFP shield the protein from the denaturing effect of the synthetic polymers (Table S2 and Figure S2, Supporting Information).

Based on our computational model that predicts an interface strongly stabilized by electrostatic interactions between complementary pairs of leucine zippers (Figure S2, Supporting Information) and SEC studies showing that LEGFP elutes as a dimer in standard PBS buffer and is more monomeric at 1 M NaCl (Figure 2A), we were able to easily form macro-oligomers by simple decreasing the ionic strength of the solution. The photoluminescence figures of the large macro-oligomers held compared to those of the dimer form (Figure 2B). In addition, macro-oligomerization degree correlated with the applied ionic strengths (Pearson's $r = -0.96$; Figure 2C). This was further confirmed by dynamic light scattering (DLS), showing that LEGFP was predominantly found in dimeric form at 150 mM NaCl, while large macro-oligomers started to form at 130 mM NaCl (Figure 2D). In addition, DLS showed a relationship between the gradual ionic strength reduction and the increase in particle size (Pearson's $r = -0.95$; Figure 2E). This became obvious to the naked eye at low NaCl concentrations (Figure 2F). DLS also confirmed the creation of macro-oligomers upon addition of 50% bPEO to LEGFP solution due to the relative decrease in ionic strength of the solution (Figure S3, Supporting Information). A better understanding of the macro-oligomers' formation came from the analysis of AlphaFold2 models of 25 possible tetramers, which produced only a few energetically viable candidates, with the best interface energy of only -2.6 kcal mol⁻¹ in contrast to the dimer interface of -6.4 kcal mol⁻¹ (Figure S4, Supporting Information) with the interaction between dimeric units possibly taking place between surface charges of the β -barrel section of LEGFP. Thus, our *in silico* results suggested that the oligomer is only possible in artificial conditions of low ionic strength. To assess the fine control of the genetically encoded oligomerization process, a LEGFP variant bearing shorter leucine zippers was designed (one less repeated unit, Figure S5, Supporting Information). The short LEGFP variant was less prone to form macro-oligomers at the same conditions and did not show the same thermodynamic figures as LEGFP in the presence of synthetic polymers used in Bio-HLEDs (Figure S5, Supporting information), indicating the need of a full-length construct to achieve on-demand macro-oligomerization mediated stabilization.

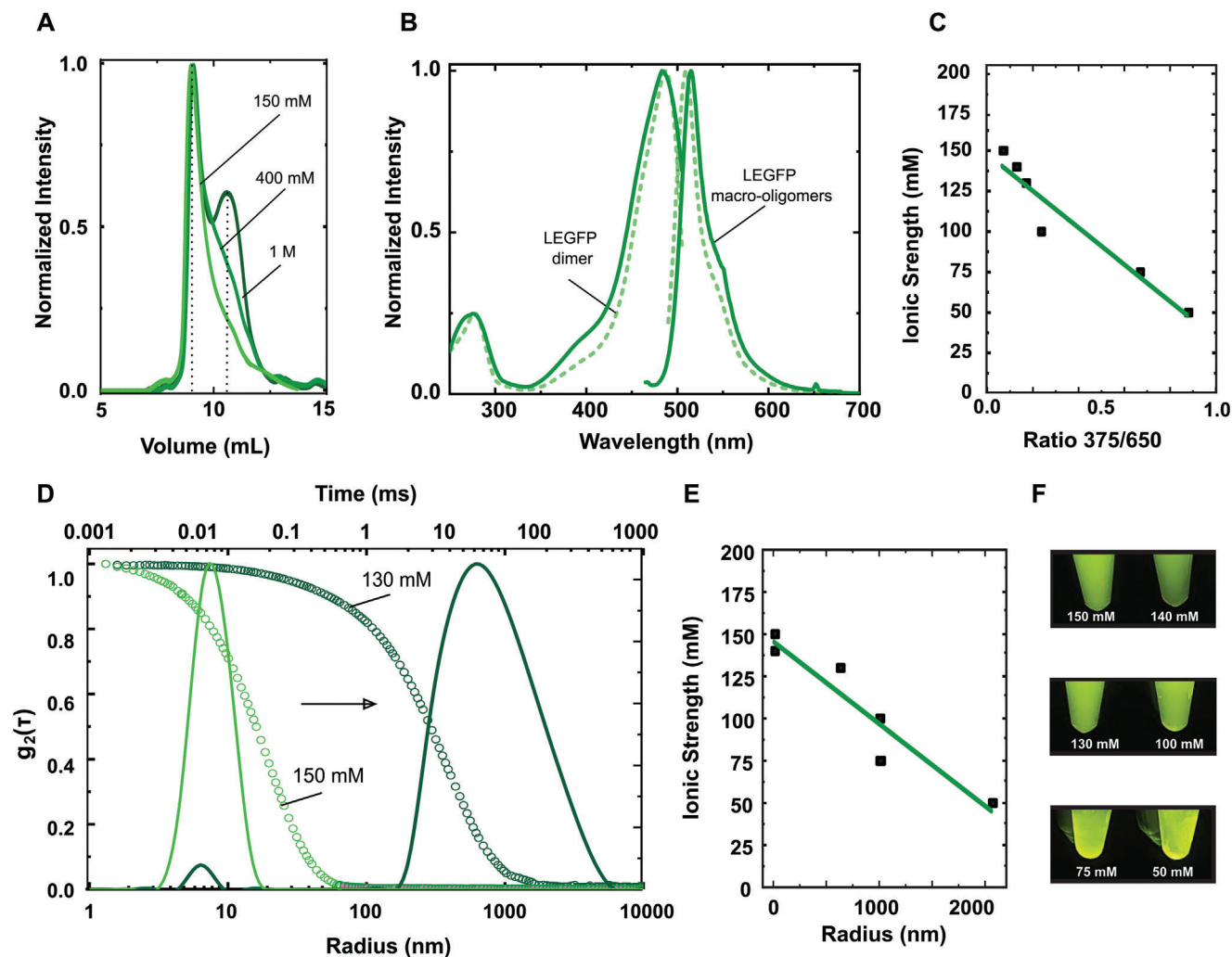


Figure 2. LEGFP dimerization and macro-oligomerization. A) SEC analysis of LEGFP upon increasing NaCl concentration, highlighting a parallel increase in LEGFP monomeric fraction. B) Comparison of excitation and emission spectra of LEGFP dimer and macro-oligomer. C) Negative correlation between ionic strength and scattering measured by UV-vis absorption spectroscopy. Macro-oligomerization is described as the intensity ratio between 375 and 650 nm. D) DLS intensity size distributions and corresponding autocorrelation functions of LEGFP measured at 150 and 130 mM NaCl. E) Negative correlation between ionic strength and radius of the macro-oligomers measured by DLS. F) LEGFP solutions at different ionic strengths under blue light (450 nm) illumination.

2.2. Benefits of Leucine-Zippers Induced Macro-Oligomerization

The superior stability of LEGFP macro-oligomers compared to their dimeric or monomeric counterparts was confirmed in a series of harsh conditions. At first, chemical denaturation using 4 M guanidinium hydrochloride was tested (Figure S6, Supporting Information), showing that the fluorescence of LEGFP macro-oligomers remained more stable over time compared to the reference EGFP and LEGFP dimer. In addition, the T_{nr} was measured changing the acetonitrile (AcN) concentrations, which is known to alter protein stability in a non-linear fashion,^[40] showing that LEGFP macro-oligomers always outperformed EGFP and LEGFP dimers (Figure 3A; Figure S6, Supporting Information). More importantly, the oligomer stability was enhanced upon increasing the AcN concentration, resulting in a fully stabilized fluorophore up to 75 °C (Figure 3B). This uncommon stability also

allowed us to study the behavior of LEGFP oligomers in the presence of concentrated polymers, which required pure organic solvents to solubilize (Figure S6, Supporting Information), showing, for example, that in the presence of AcN and 10% PMMA, LEGFP retained its emission up to 75 °C. More strikingly, LEGFP macro-oligomers re-suspended in AcN did not show a significant loss (<5%) in ϕ over the course of 2160 h (Figure 3C), while the final excitation and emission spectra slightly broadened compared to those of the macro-oligomers in MQ (Figure 3D). This goes hand-in-hand with a decrease of the τ values from 2.5 ns (0 h) to 2.3 ns (2160 h) (Figure 3E), indicating an even tighter protein macro-oligomerization^[41] after 3 months of incubation in AcN. As water and AcN are mixable, the entrapped water in the macro-oligomer structure could diffuse over time modifying the packing density. Finally, macro-oligomers were also incubated in toluene and dichloromethane (DCM), exhibiting stable ϕ and τ values

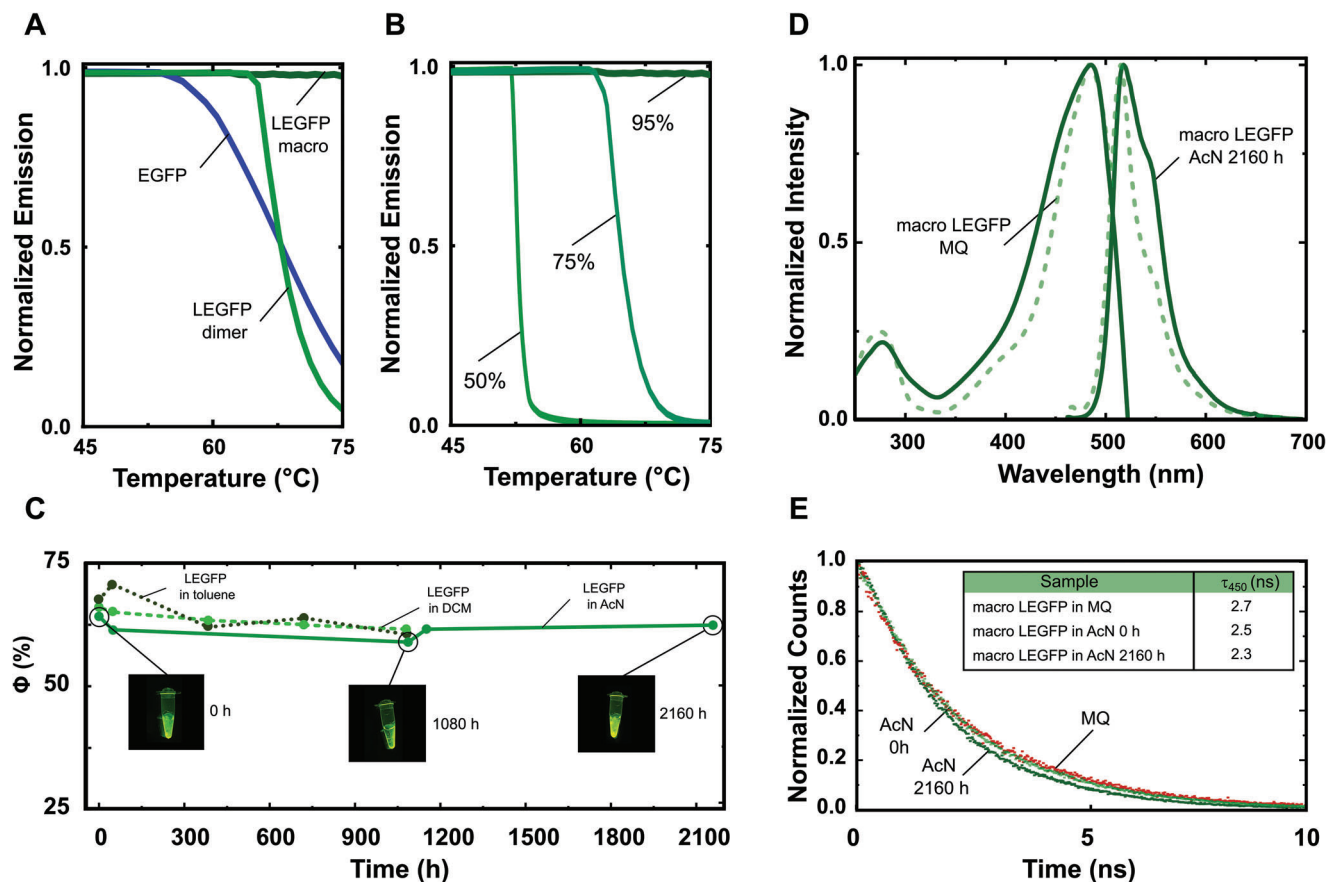


Figure 3. LEGFP macro-oligomers characterization in harsh conditions. A) T_{nr} of LEGFP macro-oligomers, dimers, and EGFP in 95% AcN. B) T_{nr} of LEGFP macro-oligomers in 50%, 75%, and 95% vt. of AcN. C) ϕ over time of LEGFP macro-oligomers in pure AcN, DCM, and toluene. D) Excitation and emission spectra of LEGFP macro-oligomers in MQ water and after 2160 h in AcN. E) τ values of LEGFP macro-oligomers in MQ water, LEGFP macro-oligomers in AcN at time 0 h, and after 2160 h of incubation.

over 1080 h (Figure 3C; Figure S6, Supporting Information). The slightly enhanced emission figures compared to those in AcN could be attributed to tight immobilization of the entrapped water inside the protein macro-oligomer structure due to the lack of solvent exchange.

Based on these results, we can state that LEGFP macro-oligomers act as a stiff protein assembly, keeping the protein in the correct folding even under harsh environmental conditions, effectively preserving the protein function. This contrasts with natural tetramerization, in which photophysical properties are commonly affected.^[42]

2.3. Reference Water-Processed Green-Emitting Devices

The Bio-HLED concept aims to replace color rare earth based down-converting filters, which are typically deposited onto the blue-LED chip by FPs embedded into polymers (water-processed mixture of a branched and linear polyethylene oxide composite),^[4–6] metal–organic frameworks,^[43,44] and biopolymers.^[45] As reference, a blue-emitting LED chip (450 nm; Winger Electronics, 1 W) was directly covered by the optimized water-processed FP-polymer down-converting filter

(dome-shaped with LEGFP macro-oligomers and EGFP [0.5 mg] in the so-called on-chip architecture; that is zero distance between LED chip and color filter). While both coatings showed a similar green emission spectra that is more red-shifted for the EGFP compared to those in solution (25 nm), the ϕ and τ figures held for LEGFP and were reduced for EGFP (Figure 4A). This is associated to the distortion in the β -barrel structure due to the dense polymeric surrounding,^[6,7] while LEGFP remained mostly unaffected due to its oligomeric character.

All the devices showed an almost full conversion ($\approx 90\%$) of the blue-emitting chip with an overall green emission (x/y CIE color coordinates of 0.25/0.50 and color purity of ≈ 80) stable in the range of the applied currents (Figure 4B). In line with the ϕ values of the color filters, the efficacy of the Bio-HLEDs with LEGFP was superior, reaching a maximum value of 94 lm W^{-1} upon increasing the applied current (Figure 4B). Concerning device stability (Figure 4C), high-power driving conditions were applied (i.e., 200 mW cm^{-2} incident photon flux excitation or 200 mA), reaching a 50% loss of the initial luminous intensity in 30 s and 24 min for devices with EGFP and LEGFP macro-oligomers, respectively. The stability difference is attributed to: i) the photon-induced heat generation process that reaches 70°C for EGFP-devices and is strongly reduced to 42°C in

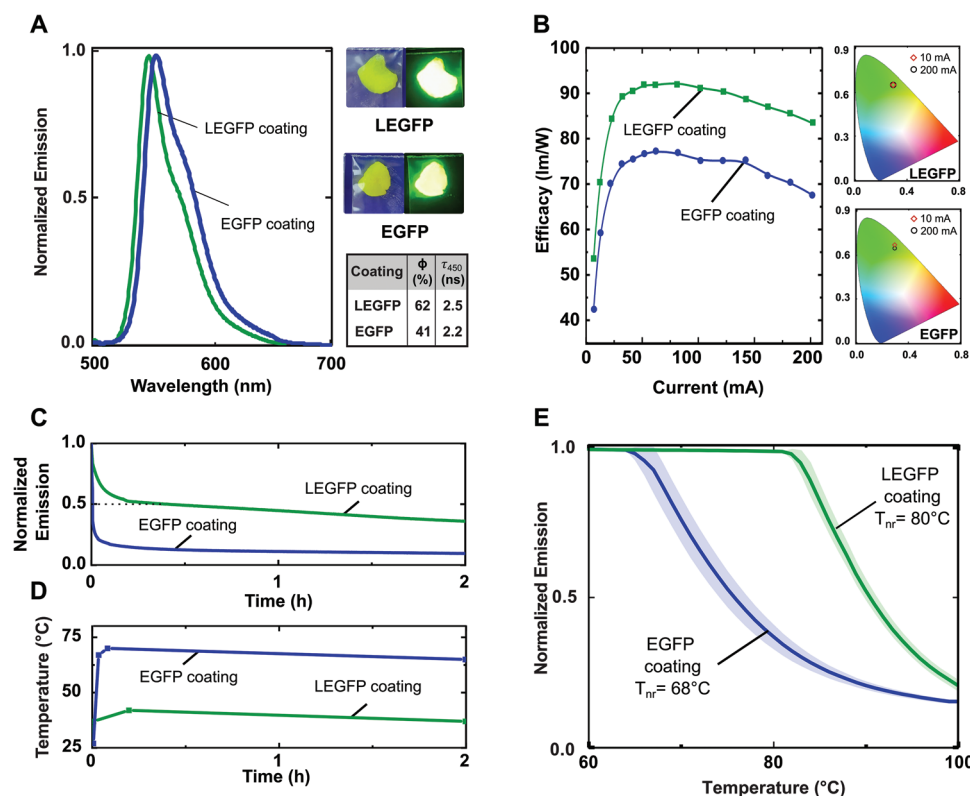


Figure 4. Reference water-processed LEGFP- and EGFP-based coatings characterization. A) Emission spectra and photophysical characterization of reference LEGFP and EGFP coatings shown on the right under room illumination (left) and blue light (right). B) Efficacy versus applied current of reference LEGFP- and EGFP-based on-chip Bio-HLEDs and their respective x/y CIE color coordinates at 10 and 200 mA, highlighting the device chromaticity stability. C) Stability and D) temperature rise of reference LEGFP- and EGFP-based coatings applied to on-chip Bio-HLEDs driven at 200 mW cm⁻². E) Non-reversibility folding temperatures (T_{nr}) of reference EGFP- and LEGFP-based polymer coatings.

LEGFP-devices (Figure 4D) because photo-induced protein motion and heat transfer to the trapped water molecules are reduced by the macro-oligomer structure^[6,7] and ii) the superior thermodynamic stability of LEGFP in the polymer coatings with a stable T_{nr} as the macro-oligomers structure effectively shields from the surrounding denaturing polymers (Figure 4E), while EGFP coatings showed a reduced T_{nr} similar to that in solution with the addition of bPEO (Figure 1H).

2.4. Water-Free Rainbow- and White-Emitting Devices

Capitalizing on the extraordinary stability of LEGFP macro-oligomers in organic solvents (vide supra), we used a commercial color down-converting filter composition based on AcN-processed PMMA coating with 5 mg of protein content and the above on-chip device architecture.^[7,46–49] In contrast to the water-processed reference coatings, the emission spectrum is slightly broader and the ϕ is slightly reduced (62 vs 57%; Figure 5A), highlighting that the oligomer structure effectively shields the FPs under these harsh processing conditions. These Bio-HLEDs showed a full conversion with a green emission (x/y CIE coordinates of 0.29/0.57 and color purity of 83) and a slightly reduced efficacy (80 lm W⁻¹; Figure S7, Supporting Information) that held at all the driving current regime. The devices were driven at the above

high-power conditions, reaching a moderate increase in temperature (<40 °C) and a remarkable stability value of 21 h (Figure 5B), representing i) one order of magnitude enhancement with respect to the best reported on-chip Bio-HLEDs with 2 h stability using an optimized EGFP variant in a bPEO:PMMA matrix and the same driving conditions^[7] and ii) two orders of magnitude enhancement with respect to on-chip HLEDs with the patented color converter dye-based BASF LUMOGEN 83 F Yellow^[7,46–49] embedded in the same PMMA matrix, which reached L50 of 7 min at the same driving conditions (Figure S8, Supporting Information).

As a final step, we turned to demonstrate the versatility of the genetically encoded oligomerization concept to other FPs to create red- and white-emitting Bio-HLEDs. Thus, we fused leucine zippers in a gift bow fashion to the N- and C- terminals of mNeptune2.5 (LmNeptune2.5) that features excellent photophysical properties for color down-conversion in protein-based lighting and is not phylogenetically close to EGFP (Figure S9, Supporting Information). Similarly to EGFP, the leucine zippers provide mNeptune2.5 with the ability to create macro-oligomers controlled by the ionic strength without affecting the protein's yield of production and emission figures, while increasing its resistance under harsh conditions (Figure S10, Supporting Information). Indeed, the emission features of the LmNeptune2.5 held constant in AcN-processed PMMA coatings (Figure 5E;

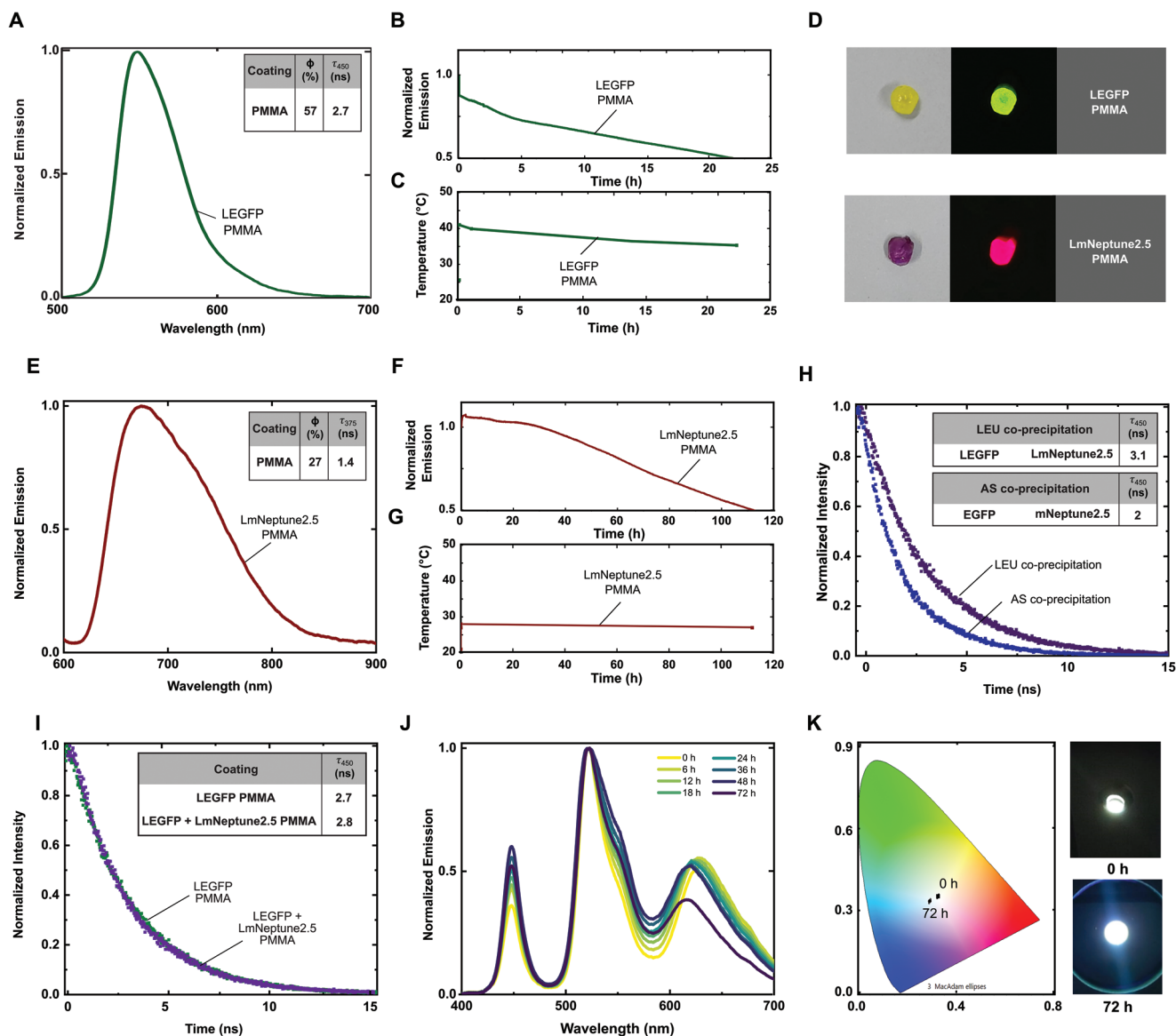


Figure 5. Water-free green-, red-, and white-emitting devices. A) Emission spectrum of Bio-HLEDs with LEGFP-PMMA coatings at a driving current of 200 mA. The inset table gathers the emission figures of the color filters. B) Stability and C) temperature reached in on-chip Bio-HLEDs with LEGFP-PMMA coatings at a driving current of 200 mA. D) Coatings under room illumination (left) and under blue light illumination (right). E) Emission spectrum of Bio-HLEDs with LmNeptune2.5-PMMA coatings at a driving current of 200 mA. The inset table gathers the emission figures of the color filters. F) Stability and G) temperature reached in on-chip Bio-HLEDs with LEGFP-PMMA coatings at a driving current of 200 mA. H) τ values of EGFP in co-precipitates with mNeptune2.5 obtained via the leucine zipper macro-oligomerization strategy and via ammonium sulfate precipitation. I) τ values of LEGFP in green- and white-emitting coatings. J, K) white emission spectra changes over time of on-chip Bio-HLEDs with LEGFP-LmNeptune2.5-PMMA at a driving current of 20 mA. Pictures of the white-emitting Bio-HLEDs at time 0 and 72 h are provided on the right.

Figure S10, Supporting Information). The on-chip Bio-HLED (590 nm; Winger Electronics, 1 W) featured a full conversion with a deep-red color (x/y CIE color coordinates of 0.73/0.26 and color purity of 85) associated to an external quantum efficiency of 1% in the applied driving currents range (Figure S11, Supporting Information). At 200 mA (55 mW cm^{-2}) driving conditions, the device did not exhibit an increase of the temperature, reaching a remarkable L50 of 110 h comparable to the prior-art.^[4,35]

White-emitting Bio-LEDs have been successfully produced using micropatterning or layer-by-layer deposition techniques.^[4,50]

However, integrating both green and red-emitting proteins in a single-coating has always been challenging due to uncontrolled FRET (Förster resonance energy transfer), which caused the higher energy component's emission to be sacrificed.^[51] Macro-oligomerization of LmNeptune2.5 and LEGFP offered a solution to this problem. Indeed, while the co-precipitation of mNeptune2.5 and EGFP using ammonium sulfate at a mass ratio that enables white emission results in a significant reduction in the τ of EGFP (Figure 5H), the co-oligomerization of LEGFP with LmNeptune2.5 at the same mass ratio showed no detectable τ

reduction, indicating the absence of FRET and the creation of macro-oligomers mainly enriched by one FP specie. In silico data confirmed that the higher-order oligomers of hybrid species containing LmNeptune2.5 and LEGFP are less energetically favorable (Table S3, Supporting Information), further validating the absence of FRET. Consequently, we could easily fabricate white-emitting coatings by a simple mixture of both types of oligomers in a single PMMA matrix. At 450 nm excitation, the emission spectrum featured the emission peaks of each protein associated with ϕ 60% and unchanged τ values for each oligomer, confirming the total absence of FRET in the PMMA matrix (Figure 5I). This led to on-chip white-emitting Bio-HLEDs (450 nm; Winger Electronics, 1 W) with a warm white emission (x/y CIE color coordinates of 0.32/0.34, color correlated temperature of 5843 K, and color rendering index of 63) at the applied current regime (Figure S12, Supporting Information). At 20 mA (40 mW cm⁻²), the device chromaticity was stable over 70 h (Figure 5J,K), comparable with the best reported Bio-HLEDs.^[3,35–37] This nicely highlights the success of our simple, versatile, and selective genetically encoded oligomerization concept to realize protein-based optoelectronics.

3. Conclusion

Proteins and enzymes have been traditionally designed and evolved to function in aqueous environments and mild stress scenarios, representing a major roadblock toward advancing protein-based optoelectronics fulfilling the green photonics concept: the further development of our current technology using eco-efficient and highly performing materials/components replacing those toxic, non-abundant, and hard-to-recycle. However, the mature knowledge to genetically modify them targeting several functionalities and to upscale their production makes them ideal candidates. In this sense, efforts to preserve protein/enzyme functions in non-aqueous environments and harsh environment conditions have typically led to low stabilities terms (a few days), a significant function loss, and lack of specificity, among others. In stark contrast to the prior-art, we have demonstrated that the leucine zipper gift bow strategy is a versatile and protein specific concept to produce LEGFP and LmNeptune2.5 macro-oligomers via electrostatic driven control, achieving remarkable function stability (emission merits preserved for >3 months) and thermal folding stability (enhanced T_m) in pure AcN, toluene, and DCM solvents, and even in the presence of synthetic polymers. This allowed us to fabricate first water-free green-, red-, and white-emitting Bio-HLEDs showing first-class performance compared to those with their respective native proteins and the prior-art (i.e., enhanced device stabilities going from a few minutes to up to \approx 100 h). Thus, macro-oligomerization applied to biological systems opens the door to develop high-end biogenic and/or bio-hybrid functional materials/components.

Supporting Information

Supporting Information is available from the Wiley Online Library or from the author.

Acknowledgements

M.P. and M.N. contributed equally to this work. R.D.C., M.P., and D.G.-A. acknowledge the European Union's Horizon 2020 research and innovation ERC-Co InOutBioLight No. 816856. M.N. and R.D.C. acknowledge FPNP-BioLED No. 101022975 funded by H2020-MSCA-IF-2020 of the European Commission, and J.A.B.-V. acknowledges AnBioLED No. 101064305 funded by HORIZON-MSCA-2021-PF-01 of the European Commission.

Open access funding enabled and organized by Projekt DEAL.

Conflict of Interest

The authors declare no conflict of interest.

Data Availability Statement

The data that support the findings of this study are available from the corresponding author upon reasonable request.

Keywords

bio-hybrid light-emitting diodes, engineered fluorescent proteins, oligomerization, organic solvent stability, protein-based lighting

Received: April 28, 2023

Revised: July 26, 2023

Published online: October 17, 2023

- [1] R. Y. Tsien, *Annu. Rev. Biochem.* **1998**, *67*, 509.
- [2] A. Miyawaki, J. Llopis, R. Heim, J. M. McCaffery, J. A. Adams, M. Ikura, R. Y. Tsien, *Nature* **1997**, *388*, 882.
- [3] Y. Zhou, S. P. Centeno, K. Zhang, L. Zheng, R. Göstl, A. Herrmann, *Adv. Mater.* **2023**, *35*, 2210052.
- [4] M. D. Weber, L. Niklaus, M. Pröschel, P. B. Coto, U. Sonnewald, R. D. Costa, *Adv. Mater.* **2015**, *27*, 5493.
- [5] V. Fernández-Luna, P. B. Coto, R. D. Costa, *Angew. Chem., Int. Ed.* **2018**, *57*, 8826.
- [6] V. Fernández-Luna, D. Sánchez-de Alcázar, J. P. Fernández-Blázquez, A. L. Cortajarena, P. B. Coto, R. D. Costa, *Adv. Funct. Mater.* **2019**, *29*, 1904356.
- [7] A. Espasa, M. Lang, C. F. Aguiño, D. Sanchez-deAlcazar, J. P. Fernández-Blázquez, U. Sonnewald, A. L. Cortajarena, P. B. Coto, R. D. Costa, *Nat. Commun.* **2020**, *11*, 879.
- [8] J. Caro-Astorga, K. T. Walker, N. Herrera, K.-Y. Lee, T. Ellis, *Nat. Commun.* **2021**, *12*, 5027.
- [9] A. M. Klivanov, *Nature* **2001**, *409*, 241.
- [10] E. M. Pelegri-O'Day, H. D. Maynard, *Acc. Chem. Res.* **2016**, *49*, 1777.
- [11] B. Panganiban, B. Qiao, T. Jiang, C. DelRe, M. M. Obadia, T. D. Nguyen, A. A. A. Smith, A. Hall, I. Sit, M. G. Crosby, P. B. Dennis, E. Drockenmuller, M. La Olvera de Cruz, T. Xu, *Science* **2018**, *359*, 1239.
- [12] M. Cortes-Clerget, N. Akporji, J. Zhou, F. Gao, P. Guo, M. Parmentier, F. Gallou, J.-Y. Berthon, B. H. Lipschutz, *Nat. Commun.* **2019**, *10*, 2169.
- [13] D. Avnir, T. Coradin, O. Lev, J. Livage, *J. Mater. Chem.* **2006**, *16*, 1013.
- [14] K. Chen, F. H. Arnold, *Proc. Natl. Acad. Sci. U. S. A.* **1993**, *90*, 5618.
- [15] J. C. Moore, F. H. Arnold, *Nat. Biotechnol.* **1996**, *14*, 458.
- [16] J.-D. Pédelacq, S. Cabantous, T. Tran, T. C. Terwilliger, G. S. Waldo, *Nat. Biotechnol.* **2006**, *24*, 79.
- [17] J. Mansfeld, R. Ulbrich-Hofmann, *Biotechnol. Bioeng.* **2007**, *97*, 672.

- [18] M. T. Reetz, P. Soni, L. Fernández, Y. Gumulya, J. D. Carballeira, *Chem-Comm* **2010**, 46, 8657.
- [19] T. Koudelakova, R. Chaloupkova, J. Brezovsky, Z. Prokop, E. Sebestova, M. Hesseler, M. Khabiri, M. Plevaka, D. Kulik, I. K. Smatanova, P. Rezacova, R. Ettrich, U. T. Bornscheuer, J. Damborsky, *Angew. Chem., Int. Ed.* **2013**, 52, 1959.
- [20] S. Petermel, J. Grdadolnik, V. Gaberc-Porekar, R. Komel, *Microb. Cell Fact.* **2008**, 7, 34.
- [21] U. Rinas, E. Garcia-Fruitós, J. L. Corchero, E. Vázquez, J. Seras-Franzoso, A. Villaverde, *Trends Biochem. Sci.* **2017**, 42, 726.
- [22] S. I. Bakhaldina, A. M. Stenkova, E. P. Bystritskaya, E. V. Sidorin, N. Y. Kim, E. S. Menchinskaya, T. Y. Gorpenchenko, D. L. Aminin, N. A. Shved, T. F. Solov'eva, *Molecules* **2021**, 26, 3936.
- [23] E. Fresta, V. Fernández-Luna, P. B. Coto, R. D. Costa, *Adv. Funct. Mater.* **2018**, 28, 1707011.
- [24] U.S. Department of Energy, 2022 Solid-State Lighting R&D Opportunities, <https://www.energy.gov/sites/default/files/2022-02/2022-ssl-rd-opportunities.pdf> (accessed: July 2023).
- [25] E. U. Commission, Energy Roadmap 2050, https://energy.ec.europa.eu/system/files/2014-10/roadmap2050_ia_20120430_en_0.pdf (accessed: July 2023).
- [26] M.-H. Fang, Z. Bao, W.-T. Huang, R.-S. Liu, *Chem. Rev.* **2022**, 122, 11474.
- [27] G. B. Nair, H. C. Swart, S. J. Dhoble, *Prog. Mater. Sci.* **2020**, 109, 100622.
- [28] C. Ezquerro, E. Fresta, E. Serrano, E. Lalinde, J. García-Martínez, J. R. Berenguer, R. D. Costa, *Mater. Horiz.* **2019**, 6, 130.
- [29] J. He, S. Yang, K. Zheng, Y. Zhang, J. Song, J. Qu, *Green Chem.* **2018**, 20, 3557.
- [30] L. Niklaus, H. Dakhil, M. Kostrzewa, P. B. Coto, U. Sonnewald, A. Wierschem, R. D. Costa, *Mater. Horiz.* **2016**, 3, 340.
- [31] N. J. Findlay, J. Bruckbauer, A. R. Inigo, B. Breig, S. Arumugam, D. J. Wallis, R. W. Martin, P. J. Skabara, *Adv. Mater.* **2014**, 26, 7290.
- [32] M. Nieddu, M. Patrian, S. Ferrara, J. P. Fuenzalida Werner, F. Kohler, E. Anaya-Plaza, M. A. Kostianinen, H. Dietz, J. R. Berenguer, R. D. Costa, *Adv. Sci.* **2023**, 10, e2300069.
- [33] S. Ferrara, J. P. Fernández-Blázquez, J. P. Fuenzalida Werner, R. D. Costa, *Adv. Funct. Mater.* **2023**, 33, 2300350.
- [34] M. Hasler, M. Patrian, J. A. Banda-Vázquez, S. Ferrara, A. C. Stiel, J. P. Fuenzalida-Werner, R. D. Costa, *Adv. Funct. Mater.* **2023**, 2301820, <https://doi.org/10.1002/adfm.202301820>.
- [35] S. Sadeghi, R. Melikov, D. Conkar, E. N. Firat-Karalar, S. Nizamoglu, *Adv. Mater. Technol.* **2020**, 5, 2000061.
- [36] B. J. Bender, A. Cisneros, A. M. Duran, J. A. Finn, D. Fu, A. D. Lokits, B. K. Mueller, A. K. Sangha, M. F. Sauer, A. M. Sevy, G. Sliwoski, J. H. Sheehan, F. DiMaio, J. Meiler, R. Moretti, *Biochemistry* **2016**, 55, 4748.
- [37] J. Jumper, R. Evans, A. Pritzel, T. Green, M. Figurnov, O. Ronneberger, K. Tunyasuvunakool, R. Bates, A. Žídek, A. Potapenko, A. Bridgland, C. Meyer, S. A. A. Kohl, A. J. Ballard, A. Cowie, B. Romera-Paredes, S. Nikolov, R. Jain, J. Adler, T. Back, S. Petersen, D. Reiman, E. Clancy, M. Zielinski, M. Steinegger, M. Pacholska, T. Berghammer, S. Bodenstein, D. Silver, O. Vinyals, et al., *Nature* **2021**, 596, 583.
- [38] Y. Teijeiro-Gonzalez, A. Crnjar, A. J. Beavil, R. L. Beavil, J. Nedbal, A. L. e Marois, C. Molteni, K. Suhling, *Biophys. J.* **2021**, 120, 254.
- [39] P. B. Crowley, K. Brett, J. Muldoon, *ChemBioChem* **2008**, 9, 685.
- [40] K. Griebenow, A. M. Klibanov, *J. Am. Chem. Soc.* **1996**, 118, 11695.
- [41] E. Clancy, S. Ramadurai, S. R. Needham, K. Baker, T. A. Eastwood, J. A. Weinstein, D. P. Mulvihill, S. W. Botchway, *Sci. Rep.* **2023**, 13, 422.
- [42] R. E. Campbell, O. Tour, A. E. Palmer, P. A. Steinbach, G. S. Baird, D. A. Zacharias, R. Y. Tsien, *Proc. Natl. Acad. Sci. U. S. A.* **2002**, 99, 7877.
- [43] P. A. Sontz, J. B. Bailey, S. Ahn, F. A. Tezcan, *J. Am. Chem. Soc.* **2015**, 137, 11598.
- [44] J. B. Bailey, L. Zhang, J. A. Chiong, S. Ahn, F. A. Tezcan, *J. Am. Chem. Soc.* **2017**, 139, 8160.
- [45] V. Fernández-Luna, J. P. Fernández-Blázquez, M. A. Monclús, F. J. Rojo, R. Daza, D. Sanchez-deAlcazar, A. L. Cortajarena, R. D. Costa, *Mater. Horiz.* **2020**, 7, 1790.
- [46] M. Mosca, F. Caruso, L. Zambito, B. Seminara, R. Macaluso, C. Cali, E. Feltn, *Integrated Photonics*, SPIE **2013**, p. 87670L.
- [47] M. Mosca, *Photonics Spectra* **2013**, 47, 60.
- [48] D. M. Hans Lichtenstein, *US20090146548A1*
- [49] W. J. Gary, *US10288233B2*, **2016**.
- [50] L. Niklaus, S. Tansaz, H. Dakhil, K. T. Weber, M. Pröschel, M. Lang, M. Kostrzewa, P. B. Coto, R. Detsch, U. Sonnewald, A. Wierschem, A. R. Boccaccini, R. D. Costa, *Adv. Funct. Mater.* **2017**, 27, 1601792.
- [51] C. F. Aguiño, M. Lang, V. Fernández-Luna, M. Pröschel, U. Sonnewald, P. B. Coto, R. D. Costa, *ACS Omega* **2018**, 3, 15829.